

FULL PAPER

Open Access



A quasi-27-day oscillation activity from the troposphere to the mesosphere and lower thermosphere at low latitudes

Hao Cheng^{1,2,3}, Kaiming Huang^{1,2,3*} , Alan Z. Liu⁴, Shaodong Zhang^{1,2}, Chunming Huang^{1,2} and Yun Gong^{1,2}

Abstract

Using meteor radar, radiosonde observations and MERRA-2 reanalysis data from 12 August to 31 October 2006, we report a dynamical coupling from the tropical lower atmosphere to the mesosphere and lower thermosphere through a quasi-27-day intraseasonal oscillation (ISO). It is interesting that the quasi-27-day ISO is observed in the troposphere, stratopause and mesopause regions, exhibiting a three-layer structure. In the MLT, the amplitude in the zonal wind increases from about 4 ms^{-1} at 90 km to 15 ms^{-1} at 100 km, which is different from previous observations that ISOs occurs generally in winter with an amplitude peak at about 80–90 km, and then are rapidly weakened with increasing height. Outgoing longwave radiation (OLR) and specific humidity demonstrate that there is a quasi-27-day periodicity in convective activity in the tropics, which causes the ISO of the zonal wind and gravity wave (GW) activity in the troposphere. The upward propagating GWs are further modulated by the oscillation in the troposphere and upper stratosphere. As the GWs propagate to the MLT, the quasi-27-day oscillation in the wind field is induced with a clear phase opposite to that in the lower atmosphere through instability and dissipation of these modulated GWs. Wavelet analysis shows that the quasi-27-day variability in the MLT appears as a case event rather than a persistent phenomenon, and has not a clear corresponding relation with the solar rotation effect within 1 year of observations.

Keywords: Quasi-27-day oscillation, Gravity waves, Convective activity, Mesosphere and lower thermosphere

Introduction

The circulation of the tropical stratosphere, mesosphere and lower thermosphere (MLT) is characterized by quasi-biennial (QBO), annual (AO), and semiannual (SAO) oscillations (Baldwin et al. 2001). In the tropics, convective activity is vigorous due to intense solar radiation, which can excite planetary-scale Kelvin and Rossby waves, and mid- and small-scale gravity waves (GWs). It is generally accepted that waves with different scales generated in the lower atmosphere play a vital role in driving QBO and SAO at different heights through their upward propagation and interaction with the background flow

(Lindzen 1981; Dunkerton 1997). Hence, oscillation and wave propagation and their intercoupling dominate the dynamical process in the tropical atmosphere.

Oscillations with intraseasonal time scales were noticed slightly later than the well-known QBO (Reed et al. 1961). Madden and Julian (1971) discovered a 40- to 50-day oscillation of the zonal wind in the tropical troposphere, which is referred to as the Madden–Julian oscillation (MJO). Afterwards, as the advancement of atmospheric sounding, oscillations with different periods were found in the tropical zonal wind and temperature, thus intraseasonal oscillation (ISO) is often extended to be quasi-periodic variations of about 20–100 days (Eckermann et al. 1997; Isoda et al. 2004). A number of observations reveal that ISOs are a prominent variability in the tropical atmosphere (Madden 1986; Eckermann et al. 1997; Kumar et al. 2007; Niranjankumar et al. 2011; Guharay

*Correspondence: hkm@whu.edu.cn

¹ School of Electronic Information, Wuhan University, Wuhan 430072, China

Full list of author information is available at the end of the article

et al. 2017). Until now, ISOs have drawn extensive attention because of not only their complex dynamics, but also their important influences on monsoons (Karmakar and Krishnamurti 2019) and cloud and precipitation (Barnes and Houze Jr 2013; Li et al. 2018). Theoretical, modeling and observational studies paid great efforts with regard to spatial structures, propagation patterns and generation mechanisms of ISOs. ISOs can propagate either eastward, showing Kelvin wave features (Yoshida et al. 1999), or westward, displaying Rossby wave characteristics (Lau and Peng 1990). Although tropical ISOs are mainly originated from convectively coupled wave dynamics, atmospheric response to independent forcing, water vapor variation, multiscale interaction, and solar irradiance are proposed to be possible mechanisms of ISO generation (Madden and Julian 1994; Zhang 2005).

When ISO generated in the tropical lower atmosphere propagates upward, its amplitude often quickly decays above the tropopause (Madden and Julian 1971; Rao et al. 2009; Guharay et al. 2014). However, some studies show that ISO may strengthen again in the upper stratosphere. Kumar and Jain (1994) suggested that ISO could propagate upward to the stratosphere from the tropical troposphere via leakage of its partial energy into the stratosphere. Ziemke and Stanford (1991) showed that strong ISO activity associated with tropical Rossby waves in the lower atmosphere of the Southern Hemisphere (SH) could propagate to the upper stratosphere by refracting out to mid-latitudes and then refracting back to the equatorial stratopause region, and a similar phenomenon in the Northern Hemisphere (NH) was inferred based on rocketsonde and radiosonde observations (Nagpal et al. 1994). Numerical investigation demonstrated that Rossby waves forced by the induced heating on the equator could radiate poleward into the extratropical westerlies and vertically into the stratosphere in the two hemispheres (Salby et al. 1994). Furthermore, Huang et al. (2015) presented that an ISO with relatively short period of 27 days could penetrate extreme temperature region around the tropopause and weak westward wind field in the lower stratosphere to propagate upward into the MLT, while an ISO with long period of about 46 days does not so.

In the MLT, ISOs with a wide period range of 20–60 days were reported in the zonal wind over Christmas Island (2° N, 157° W) based on medium frequency (MF) radar observation (Eckermann and Vincent 1994). The study indicated that it is unlikely that the ISOs propagate up to the MLT from the lower atmosphere although they were suggested to originate from in the lower atmosphere. Instead, Eckermann et al. (1997) proposed that GWs and tides modulated by ISOs in tropical convection could induce in turn similar periodicities in the zonal

flow of the MLT by transferring their momentum and energy into the mean flow as these waves propagate up to the MLT. Similarly, planetary waves (PWs) in the MLT are suggested to be possibly generated through momentum forcing associated with breaking GWs that have been filtered by the stratospheric mean flow modified by strong planetary waves (PWs), which is confirmed by numerical studies (Smith 2003; Sato and Nomoto 2015). Based on three radar observations in the equatorial MLT, Isoda et al. (2004) argued that nonmigrating tides modulated at ISO period in the lower atmosphere drive the variation of the zonal mean wind, but the contribution of GWs to ISO in the MLT is unclear. Satellite and Atmospheric Infrared Sounder (AIRS) measurements indicate that stratospheric GWs display an intraseasonal variability due to a critical level filtering of upward propagating GWs by the MJO wind in the troposphere (Moss et al. 2016; Tsuchiya et al. 2016). However, at mid and high latitudes, Pancheva et al. (2003) noticed an obvious ISO in the MLT from meteor radar data, but there was not a corresponding periodicity in atmospheric wave activity, including GWs, tides and quasi-2-day PWs. Similarly, by combining observations of mesosphere–stratosphere–troposphere (MST) radar and meteor radar, Huang et al. (2019) found that an ISO in the MLT at mid-latitudes was related to polar dynamical process in winter rather than wave activity. Hence, the origin of ISOs in the MLT is not very clear though many generation sources in the lower atmosphere have been suggested.

As a distinct oscillation, quasi-27-day ISO has attracted much interest because this variability is not only the same as solar rotation period but also a possible normal mode of the atmosphere. Similar to the response of ozone in the upper stratosphere to solar rotation through physicochemical mechanisms, the presence of quasi-27-day oscillation in the ionospheric variability is a natural event as solar radiation is a major source of energy and ionization (Pancheva et al. 1991; Rich et al. 2003; Xu et al. 2011; Coley and Heelis 2012). In the neutral atmosphere from the troposphere to the MLT, quasi-27-day periodicity is often observed in the zonal wind, temperature, and trace gases at different heights (Fioletov 2009; Huang et al. 2015; Hood 2016; Guharay et al. 2017; Thiéblemont et al. 2018). Although trace gases have a clear response to solar 27-day cycle, the attribution of 27-day periodicity in the atmosphere to a solar cause is complicated by the fact that internal variability of the atmosphere can itself also generate quasi-27-day oscillation (Hoffmann and von Savigny 2019). Both chemistry–climate model (CCM) and whole atmosphere community climate model (WACCM) results show that a 27-day variability in the wind and temperature is an inherent feature of the atmosphere, thus is not necessarily related to the solar rotational

period since the CCM and WACCM can output quasi-27-day variation even without solar rotational forcing (Schanz et al. 2016; Sukhodolov et al. 2017). Therefore, more observational investigations are required to reveal the origin and active features of quasi-27-day variability in the neutral atmosphere, especially in the MLT.

In this work, we report a quasi-27-day ISO activity in the tropics, which exhibits the characteristic of triple-layer structure from the troposphere to the MLT. “Data” section covers a brief explanation of the data that we utilized. In “Quasi-27-day oscillation” section, we investigate the features of the quasi-27-day variability throughout the troposphere to the MLT. “Discussion” section discusses the origin of the oscillation in the lower atmosphere and the possible relation among different atmospheric layers, and a summary is presented in “Summary” section.

Data

Meteor radar observation

The horizontal wind from a meteor radar located in Kihei on Maui, Hawaii, at 20.75° N, 156° W, is used in the study. The radar system is an all-sky interferometric meteor (SKiYMET) radar operating at a frequency of 40.92 MHz. A 3-element Yagi antenna pointing to zenith transmits a peak power of 6 kW at a 13.3 μ s pulse length to illuminate meteor trails. Five 3-element Yagi antennas oriented along two orthogonal baselines receive echoes from meteor trails in a 13.3 μ s sampling time, resulting in a height resolution of 2 km. The horizontal wind velocities are derived from Doppler shifts by moving meteor trails within a height range of 4 km and a time bin of 1 h, and then the hourly wind profile is obtained by oversampling at a 1 km height interval in the range from 80 to 100 km. A technical description of SKiYMET radar can be found in the work of Hocking et al. (2001), and the Maui meteor radar system and the wind computation are presented in detail by Franke et al. (2005). The number of meteor counts detected by the radar showed a strong dependence on altitude, with an approximate Gaussian distribution centered at about 90 km, thus the wind measurement errors are small with typical values of 3–4 ms^{-1} around 90 km. As the height increases or decreases, the detection number of meteors decreases, and then the statistical uncertainties of wind gradually increase, and may be more than 10 ms^{-1} at 80 and 100 km sometimes. In the wind calculation, horizontal wind vectors were estimated in the chosen time–height bin when at least six meteor echoes are available and the RMS uncertainty of the radial velocity is less than 7 ms^{-1} (Franke et al. 2005). In the 81-day period of our concern, the acceptance rate of wind data attains about 90% at 98 km, and these missing observations are replaced with linearly interpolated data.

Franke et al. (2005) compared the zonal and meridional winds between the meteor radar and Na Doppler lidar observations in Kihei, which shows a good consistency between the radar and lidar measurements at the common coverage altitudes. The meteor radar observation has been applied to investigating dynamical processes in the MLT over Maui (Liu et al. 2013; Huang et al. 2013a, b).

The radar system is under maintenance from 26 October 2005 to 12 April 2006, thus we choose the zonal wind at the height of 100 km for 1 year from 13 April 2006 to 12 April 2007, to examine the temporal activity of quasi-27-day oscillation throughout the year. The horizontal wind data for 81 days from 12 August to 31 October 2006 is utilized to study the vertical evolution of the quasi-27-day ISO in the MLT.

Radiosonde observation

The United States radiosonde observations at three tropical stations distributed in the NH and SH are applied to the analysis of the oscillation activity in the troposphere and lower stratosphere. The data are archived and provided freely by the National Climatic Data Center (NCDC) of National Oceanic and Atmospheric Administration (NOAA) through the Stratospheric Processes and Their Role in Climate (SPARC) Data Center at <ftp://ftp.ncdc.noaa.gov>. The three stations are located in Hilo (19.72° N, 155.07° W), Kauai (21.98° N, 159.35° W) on Hawaii, and in Pago Pago (14.33° S, 170.72° W) on Samoa. Observational sites are sparse in the Pacific, thus we choose the radiosonde stations as close as possible to the meteor radar station.

The type of radiosonde is the Väisälä RS92-GDP, and routine radiosondes are usually launched twice daily at 00:00 and 12:00 UT. As a balloon rises, atmospheric horizontal wind, temperature, pressure, and relative humidity are sensed by balloon-borne platform. The sampled height depends on the ascent rate of the balloon, ranging from 10 to 100 m. At this height resolution, the temperature uncertainty is less than 0.1 K, and the horizontal wind uncertainty is smaller than 0.5 ms^{-1} . For convenience, we interpolate the raw data linearly to a uniform interval of 50 m. The maximum height of radiosonde observation is the balloon burst altitude. In the period that we focus on, about 90%, 88% and 90% of balloons reached 30 km in Hilo, Kauai and Pago Pago, respectively, but only about 63%, 87% and 87% attained 31 km. Hence, we select the altitude of 30 km as the upper height limit of radiosonde observation in our analysis.

We follow the method proposed by Alduchov and Eskridge (1996) to derive specific humidity from temperature, pressure and relative humidity measured by radiosonde.

OLR and index of solar activity

Specific humidity and outgoing longwave radiation (OLR) have often been used as proxies of convective activity over the tropical region (Arkin and Ardanuy 1989). We expect to explore the origin of the tropical oscillation by combining specific humidity and OLR. Daily OLR data are obtained from the NOAA at the website of <https://www.esrl.noaa.gov/psd>, with a 2.5° latitudinal and longitudinal resolution (Liebmann and Smith 1996).

We also examined solar forcing as potential controlling factors of the atmosphere. Daily solar 10.7 cm radio flux (F10.7) and Lyman- α flux are used as a measure of solar activity. The F10.7 data are accessed from the National Centers for Environmental Information (NCEI) of NOAA at the website of <https://www.ngdc.noaa.gov>, and the Lyman- α flux data are downloaded from Laboratory for Atmospheric and Space Physics (LASP), University of Colorado at <http://lasp.colorado.edu/lisird>. The measurement was taken during the late declining phase of solar cycle 23.

Reanalysis data

The Modern-Era Retrospective Analysis for Research and Applications (MERRA) reanalysis of the National Aeronautics and Space Administration (NASA) is an ideal candidate to investigate the features of the oscillation in the zonal, meridional and vertical directions. The product of “inst6_3d_ana_Nv” in the version 2 of MERRA (MERRA-2) is available through the NASA Goddard Earth Sciences Data and Information Services Center (GES DISC) online archive at <https://disc.gsfc.nasa.gov/datasets>. The reanalysis data is 6-hourly instantaneous analysis fields on a $0.5^\circ \times 0.625^\circ$ latitude-by-longitude grid at 72 model levels from ground up to 0.01 hPa (Gelaro et al. 2017).

In this study, the data of F10.7, Lyman- α flux and zonal wind at 100 km are used for 1-year data from 13 April 2006 to 12 April 2007, which are identified by month. The other data used are in the same period from 12 August to 31 October 2006, and 12 August 2006 is referred to as day 1.

Quasi-27-day oscillation

Oscillation in MLT

Figure 1 shows the daily averaged zonal and meridional winds measured by the meteor radar for 81 days from 12 August to 31 October 2006. The mean zonal wind (positive eastward) has a maximum of 50.7 ms^{-1} at 95 km on day 59 and a minimum of -67.0 ms^{-1} at 100 km on day 24, while the mean meridional wind (positive northward)

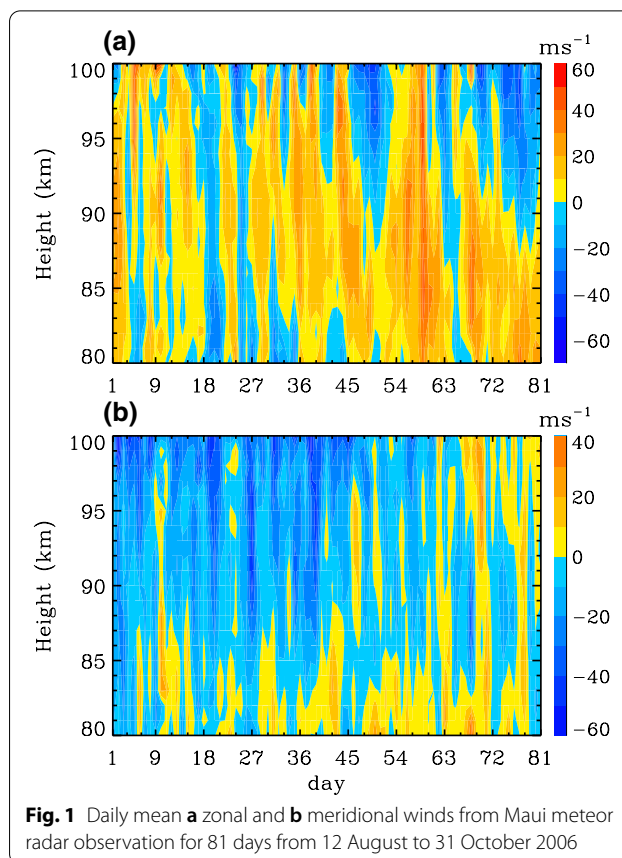
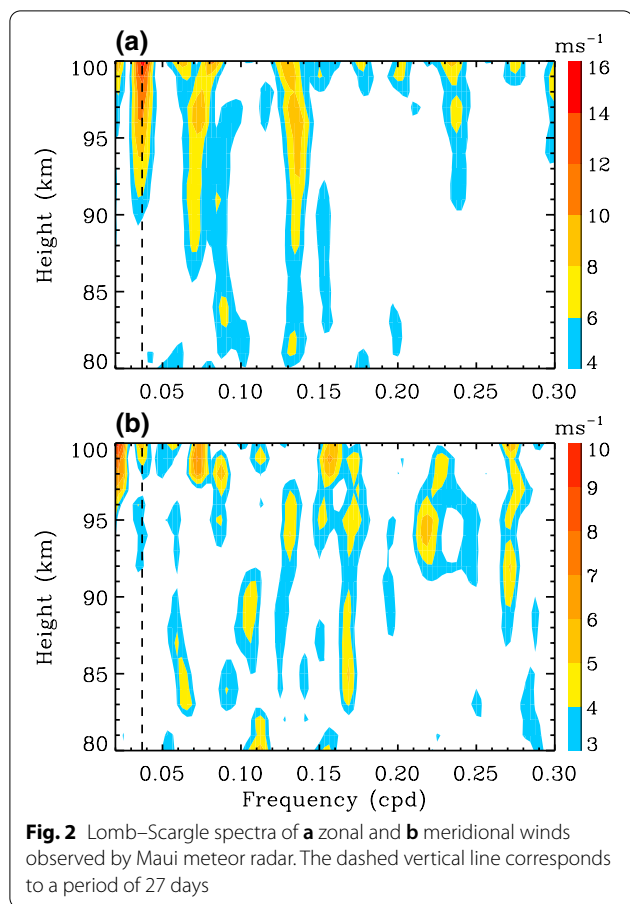


Fig. 1 Daily mean **a** zonal and **b** meridional winds from Maui meteor radar observation for 81 days from 12 August to 31 October 2006

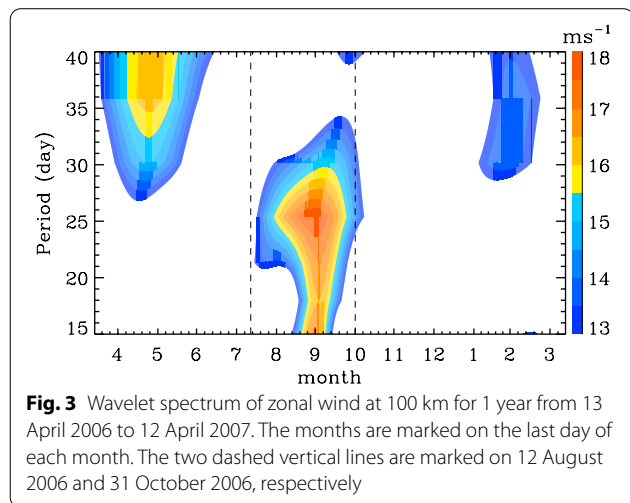
is between -59.3 and 40.0 ms^{-1} . The different temporal scale perturbations can be seen in the wind field.

We carry out a Lomb–Scargle spectrum analysis (Scargle 1982), with a 4-time oversampling, on the daily averaged zonal and meridional winds to investigate their spectral components. Figure 2 shows the Lomb–Scargle spectrum of the mean zonal and meridional winds. A confidence level of 95% corresponds to a spectral amplitude of 7.4 ms^{-1} . It is interesting that the spectral components in the zonal wind are very weak below 90 km, while above 90 km, a quasi-27-day oscillation is a predominant component, and strengthens gradually with height. Its spectral amplitude grows to 15.2 ms^{-1} at 100 km from 4.2 ms^{-1} at 90 km. The quasi-27-day periodicity also arises in the meridional wind and shows a similar vertical variation but with a weak spectral magnitude. This is consistent with early observations that atmospheric oscillation occurs mainly in the zonal wind (Eckermann et al. 1997; Luo et al. 2001; Huang et al. 2015; Guharay et al. 2014), thus we will concentrate on the zonal wind oscillation.

In order to recognize the feature of quasi-27-day oscillation throughout the year, we chose the zonal wind at 100 km for 1 year to make a wavelet transform since the



oscillation is the strongest at this height. Morlet wavelet function which consists of a plane wave modulated by a Gaussian envelope is chosen as mother wavelet. Wavelet analysis decomposes a time series into a two-dimensional time–frequency domain, thus it can provide not only the

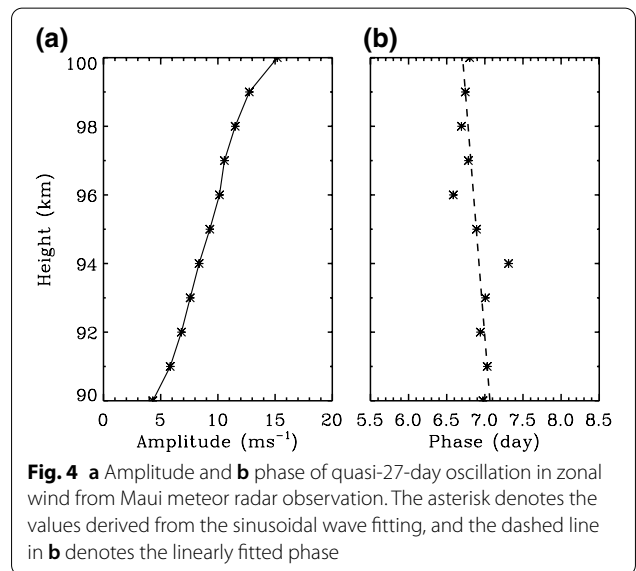


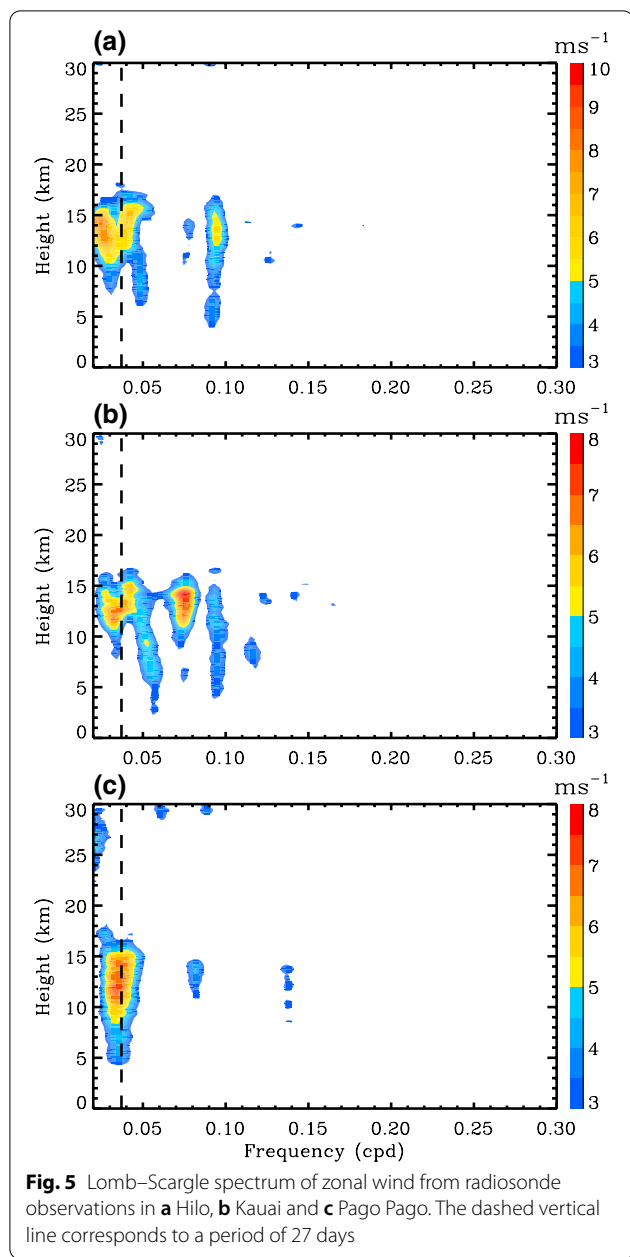
dominant components, but also the variation of these components with time. Figure 3 shows the wavelet spectrum of the zonal wind in 1 year of observation, which illustrates that the significant quasi-27-day oscillation occurs in the MLT as a case event rather than a persistent phenomenon, and only takes place once in the 1-year observation. Similarly, two MJO events arise in April–June, 2006, and February–March, 2007, respectively. The time between the two dashed vertical lines is the duration of our concern presented in Figs. 1 and 2.

In order to determine the vertical propagation of the quasi-27-day oscillation, a sinusoidal wave fit under a 27-day period is applied to the time series of the mean zonal wind for the 81-day observation at 90–100 km. The fitted amplitude and phase are shown in Fig. 4. Here, the phase is described by the time when the oscillation attains its maximum value (Huang et al. 2015). It can be seen from Fig. 4 that the amplitude of the oscillation gradually increases from 4.3 ms⁻¹ at 90 km to 15.2 ms⁻¹ at 100 km, which is in good agreement with the spectral result in Fig. 2. A linear fit of the phase exhibits a slowly downward phase progression of the oscillation in the MLT.

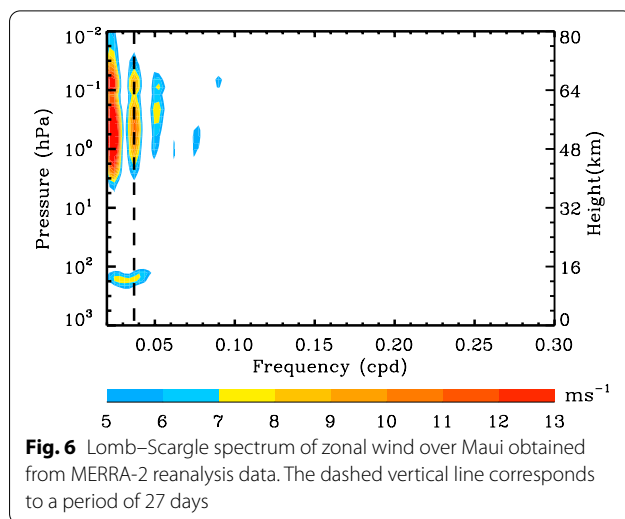
Oscillation in troposphere and stratosphere

We use the radiosonde observations and MERRA-2 reanalysis data to examine the activity of the quasi-27-day ISO in the troposphere and stratosphere. Figure 5 presents the Lomb–Scargle spectrum of the zonal wind by the radiosonde observations in Hilo and Kauai on Hawaii, and Pago Pago of the SH. The low-frequency ISOs are predominant at all the three tropical stations, whereas the evolution of the oscillations is interesting





in the source region of the troposphere. A quasi-27-day oscillation and an MJO are distinguishable in Hilo, and seem to be integrated as one with a wide period range of about 25–35 days in Kauai. Similar scenario also occurs in Pago Pago but with larger magnitude and height coverage. Hence, the oscillation shows to some extent the local characteristics, which is possibly related to the source feature and the background condition at different stations. In addition, a relatively weak quasi-10-day component arises only at the two stations of the NH. Above 17 km, there is no significant spectral peak, indicating



that it is difficult for the oscillation to penetrate through the tropopause region into the lower stratosphere. This is consistent with rapid attenuation of ISOs above the tropopause presented in many early observations (Madden and Julian 1971; Ziemke and Stanford 1991; Rao et al. 2009; Niranjankumar et al. 2011; Guharay et al. 2014).

In order to extend zonal wind information to higher altitudes, Fig. 6 plots the Lomb–Scargle spectrum of the zonal wind above Maui from the MERRA-2 reanalysis. The right vertical axis marks the approximate heights of the pressure levels derived from logarithmic pressure–height formula. The spectral feature below 10 hPa (~32 km) in the reanalysis data is roughly consistent with that in the radiosonde observations. In the reanalysis data, the quasi-27-day ISO and MJO hold the group together in the upper troposphere with a peak intensity similar to the radiosonde measurements in Hilo and Kauai. Above 36 km of the stratosphere, the two oscillations reappear and are separated from each other. The quasi-27-day component has the maximum spectral amplitude of 11.2 ms⁻¹ at 0.48 hPa (~53 km) level. It is interesting that these spectral components are weakened in the stratopause region (~60 km), and then are rapidly attenuated from about 70 km of the lower mesosphere. There is not a significant magnitude of the quasi-27-day oscillation at about 80 km, which is in agreement with the meteor radar observation. Based on the radar observation, this oscillation is strengthened above 90 km again, as shown in Fig. 2. Hence, the quasi-27-day oscillation exhibits a three-layer structure from the troposphere to the MLT over Maui.

To examine the latitudinal change of the quasi-27-day oscillation, we make a sinusoidal wave fit with a 27-day period on the zonal wind at 176.93 and 0.48 hPa (~12

and 53 km) levels along the 156.25° W longitude based on the MERRA-2 reanalysis data for the 81 days. The two pressure levels are chosen because the quasi-27-day component is strong at the two levels, as shown in Fig. 6. Figure 7 presents the evolutions of the fitted amplitude and phase with latitude. The phase variation with latitude seems to show a tendency of the oscillation propagation from the SH to the NH. The amplitudes have several extreme values between 25° S and 25° N, especially the maximal values around 20° S and 20° N at 176.93 hPa. In that case, we presented the spectrum of the zonal wind from the radiosonde observation in Pago Pago of the SH. It can be noted from Figs. 5 and 7 that the quasi-27-day ISO in the troposphere is more prominent above Pago Pago than above Hilo and Kauai. Therefore, the oscillation is present at low latitudes in the both hemispheres.

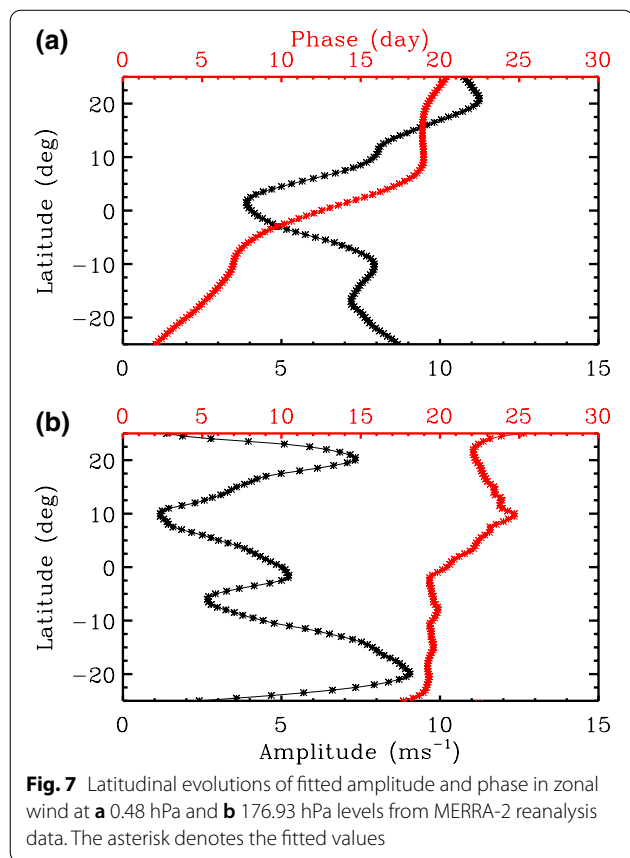
Discussion

In early studies, by using over 5 years of wind data acquired by MF radar at Christmas Island, Eckermann et al. (1997) showed that the ~60-day ISO in the zonal wind of the MLT is relatively strong in winter–early spring (December–April). Its amplitude reaches a peak of about 10–15 ms⁻¹ at 80–85 km, and then clearly

decreases with height. Similarly, based on 20-year radar observations at four sites from 30 to 70° N, the investigation indicated that the oscillation with period between 20 and 40 days at mid- and high-latitudes is active in winter (November–March), with a strength reduction from about 10 ms⁻¹ at 75–85 km to about 5 ms⁻¹ at about 100 km (Luo et al. 2001). Huang et al. (2015) exhibited a quasi-27-day oscillation in December 2004 to March 2005 over Maui with large amplitudes throughout the MLT. Its amplitude has a maximum value of 20.3 ms⁻¹ in the zonal wind at 89 km, and then monotonously drops to 7.5 ms⁻¹ at 96 km. Hence, these observational studies indicate that the ISOs in the MLT are generally robust in the heights of 80–90 km during winter. In the paper, the quasi-27-day ISO occurs during August–October, and has not a significant intensity between 80 and 90 km but is quickly strengthened from 90 to 100 km, which is different from those in the previous studies (Eckermann et al. 1997; Luo et al. 2001; Huang et al. 2015).

Since the quasi-27-day oscillation in the MLT does not come from the direct propagation from the lower atmosphere, we investigate the GW activity based on the radiosonde observations in Hilo, Kauai and Pago Pago according to ISOs driven by wave coupling among the different atmospheric layers (Eckermann and Vincent 1994; Eckermann et al. 1997). The GW perturbations are analyzed separately at 1–9 km of the troposphere and at 20–28 km of the lower stratosphere, which is for three reasons: (1) avoiding the sharp variations of the zonal wind and temperature from the upper troposphere to the lower stratosphere; (2) the small change in buoyancy frequency for each chosen height range; and (3) examining the GW features in the convective source region of 1–9 km and in the propagation region of 20–28 km.

We follow the analysis technique of Allen and Vincent (1995) and Vincent and Alexander (2000) to derive the GW perturbations from the profiles of radiosonde sounding. Assuming that the observed zonal wind, meridional wind and temperature [*u*, *v*, *T*] mainly consist of the background [\bar{u} , \bar{v} , \bar{T}] and GW perturbations [*u'*, *v'*, *T'*], we estimate the background [\bar{u} , \bar{v} , \bar{T}] by fitting a second-order polynomial to the vertical profiles of [*u*, *v*, *T*] in the chosen height interval. This second-order polynomial fitted background was widely used in GW analysis from radiosonde observations (Allen and Vincent 1995; Vincent and Alexander 2000; Zhang and Yi 2007; Huang et al. 2018), which can reduce the effect of long vertical wavelength waves. The total fluctuation quantities are obtained from the observed profiles by removing the fitted background. In order to remove fluctuations due to smaller-scale effects, such as measurement error, drag variation of balloon, noise introduced by the interpolation process (Zhang et al. 2012), we apply a high-pass filter to extract



the GW components from the total fluctuation. The cut-off wavelength of the filter is selected to be 0.5 km since lots of observations show that the vertical wavelengths of GWs are in general more than 0.5 km (Ogino et al. 1998; Yamanaka et al. 1996). The total energy per unit mass (E) is used as a measurement for GW activity, which is written as follows (Allen and Vincent 1995; Vincent and Alexander 2000):

$$E = \frac{1}{2} \left[\overline{u'^2} + \overline{v'^2} + \frac{g^2 \overline{T'^2}}{N^2} \right], \quad (1)$$

where $\widehat{T'} = \frac{T'}{T}$ is the normalized temperature perturbation; g is the acceleration due to gravity; N is the buoyancy frequency; and the overbar means an unweighted average over height. The vertical wind perturbation of GWs is neglected in Eq. (1) because there is no vertical wind in radiosonde observation, and the vertical wind perturbation of GWs is much smaller than their horizontal wind perturbation (Ratnam et al. 2009; Tsuda et al. 2009).

We derive the total energy of GWs from the observed profiles of radiosonde in Hilo, Kauai and Pago Pago during the same period of 81 days, and then calculate the daily averaged energy in Pago Pago of the SH and

between the two stations of the NH, respectively, for the sake of reducing the impact of chance events. Figure 8 shows the wavelet spectra of daily mean GW energies in the height ranges of 1–9 km of the troposphere and 20–28 km of the lower stratosphere in the NH and SH. One can note from Fig. 8 that a quasi-27-day oscillation of GW energy, with a wide spectral range, occurs in both the troposphere and the lower stratosphere. Although the quasi-27-day periodicity does not appear in the lower stratospheric wind field, its spectra around the 27-day period in the GW energy is sharper in the lower stratosphere than in the troposphere, which may be due to the filtering effect by the quasi-27-day variation in the tropospheric wind field (Moss et al. 2016; Tsuchiya et al. 2016), as shown in Fig. 5. Therefore, the GW energy investigation seems to support the coupling mechanism that GWs modulated by oscillation in the lower atmosphere induce the similar periodicity in the MLT through their energy and momentum transport (Eckermann and Vincent 1994; Eckermann et al. 1997).

As for the ISO enhancement in the upper stratosphere again, there are two possible mechanisms proposed in previous studies. Kumar and Jain (1994) argued that ISO propagates directly upward to the stratosphere from the tropical troposphere through partial energy transmission, and Huang et al. (2015)

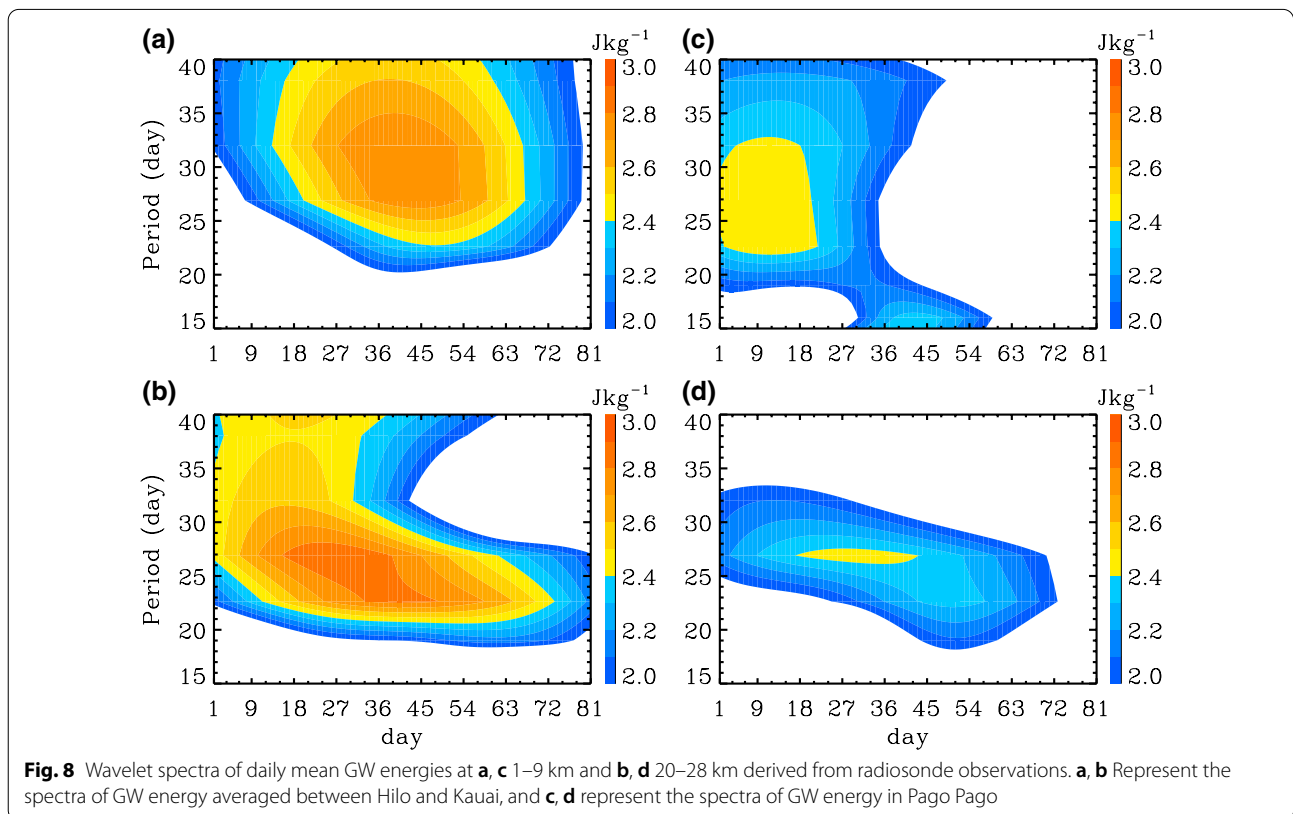
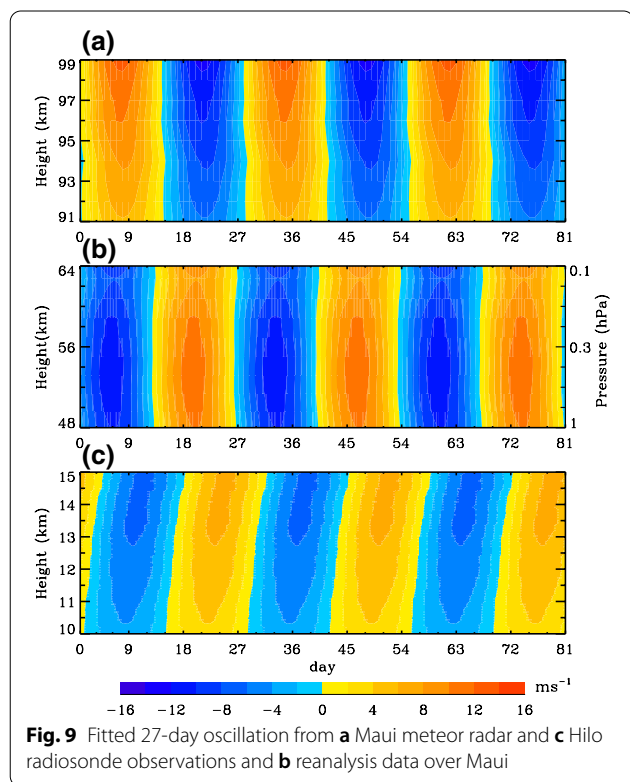
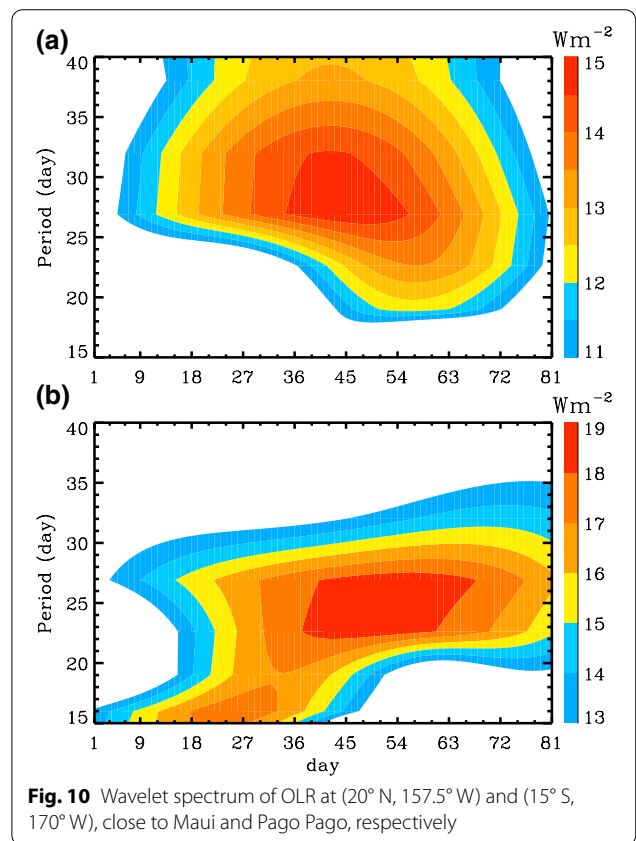


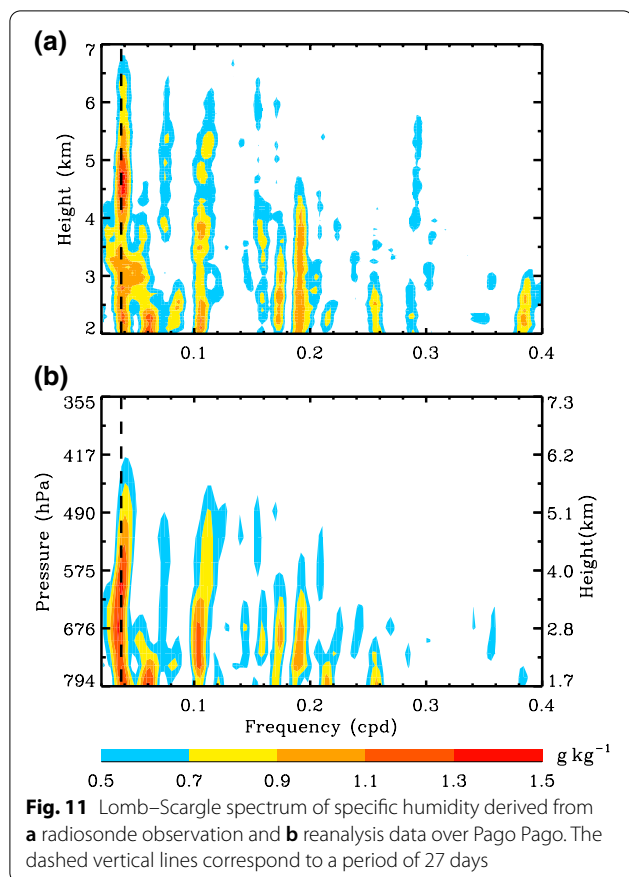
Fig. 8 Wavelet spectra of daily mean GW energies at **a, c** 1–9 km and **b, d** 20–28 km derived from radiosonde observations. **a, b** Represent the spectra of GW energy averaged between Hilo and Kauai, and **c, d** represent the spectra of GW energy in Pago Pago

confirmed the ISO penetration into the stratosphere based on the radiosonde observation. Ziemke and Stanford (1991) suggested that upward propagating ISO is refracted to mid-latitudes, and then refracted back into the tropical upper stratosphere. The phase in the stratosphere shown in Fig. 7a implies that the oscillation in the upper stratosphere propagates towards the NH low latitudes from the NH and SH mid-latitudes. In addition, the quasi-27-day ISO may be partially attributable to the GWs. As the GWs propagate to the upper stratosphere, the quasi-27-day oscillation may be enhanced by absorbing the GW momentum and energy at the critical level, and this also means that the GWs are modulated further over there. And then the modulated GWs propagate upward to higher altitudes and induce the quasi-27-day variability in the mesopause region due to their instability. In this way, the phase of the quasi-27-day ISO in the MLT should be approximately opposite to that in the lower atmosphere. Figure 9 shows the fitted 27-day oscillation in the three regions based on the Maui meteor radar and reanalysis and Hilo radiosonde data. The fitted results from the radiosonde observation in Kauai and Pago Pago (not presented) are almost the same as that in Hilo, with a peak amplitude of about 7–8 ms⁻¹. Figure 9 demonstrates the opposite phase relation between the quasi-27-day ISO in the MLT and in the lower atmosphere.



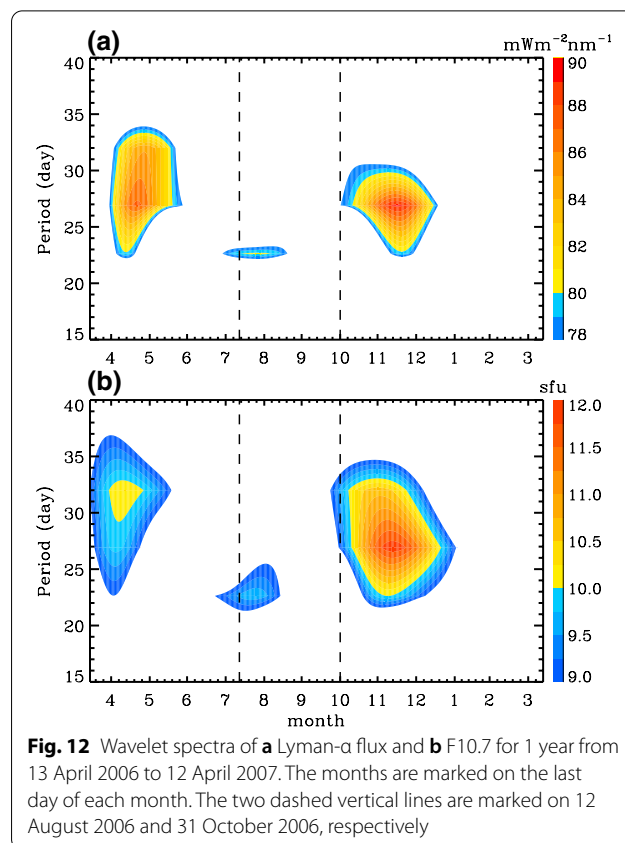
Earlier studies discussed possible mechanisms of ISO generation (Zhang 2005). It is generally recognized that ISOs in the tropics originate mainly from convective activity. OLR is often used as a proxy of convection activity. We chose the OLR data at the locations of (20° N, 157.5° W) and (15° S, 170° W), close to Maui and Pago Pago, to examine the convective activity. A wavelet transform on the OLR is carried out, which is shown in Fig. 10. It can be seen that the ISO activity in the OLR exhibits a broad period range between 20 and 40 days but with a dominant period around 27 days. We also calculate the specific humidity from the radiosonde observation in Pago Pago. Figure 11 shows the Lomb–Scargle spectrum of the specific humidity from the radiosonde measurement and the reanalysis data above Pago Pago. The spectra of specific humidity between the observation and reanalysis data are consistent with each other. The quasi-27-day periodicity is the dominant component in the water vapor variation, and the spectral analysis above 7 km (not presented here) indicates that the dominant 27-day component extends all the way to the tropopause region. The previous study by Kumar et al. (2007) showed that a 50- to 70-day ISO in the zonal wind of the tropical MLT has similarities with the oscillation of OLR, while a 20- to 40-day ISO displays similarities with the





tropospheric water vapor activity. Here, the periodicity in both the OLR and water vapor demonstrates that there is a quasi-27-day variability in the convective activity in the tropics. Since convections are a main source of tropical waves and ISOs (Fritts and Alexander 2003; Zhang 2005; Sato et al. 2009), their variability can lead to the quasi-27-day ISO not only in the zonal wind, but also in the GW activity in the tropical troposphere. When the GWs generated in the convection source region propagate upward, they are further modulated by the quasi-27-day oscillation of the zonal wind, resulting in a more prominent 27-day periodicity of the GW activity in the stratosphere than in the troposphere, as shown in Fig. 8.

We investigate whether or not solar radiation is directly responsible for the 27-day variability at high altitudes due to the absorption of solar radiation by OH, oxygen atom and ozone. Here, the Lyman- α flux and F10.7 are chosen as proxies for solar radiation, and Fig. 12 depicts that the wavelet spectra of the Lyman- α flux and F10.7 in 1 year from 13 April 2006 to 12 April 2007. One can see from Fig. 12 that the predominant variabilities in the Lyman- α flux and F10.7 are nearly consistent with each other since both of them originate



from the solar activity. The wavelet spectra illustrate two obvious quasi-27-day activities in the 1-year data. One takes place in April–June, 2006, and the other arises in November–December, 2006. However, there is no corresponding occurrence of quasi-27-day variability in the wind field of the MLT in these two time periods, as shown in Fig. 3. In April–June, 2006, the MJO in the zonal wind has a much larger dominant period than the quasi-27-day oscillation in the two solar radiation fluxes. In the duration of our concern, a rather weak quasi-22-day component in the solar radiation appears in the early period. Similar study indicated that the proposed connection between 27-day variability in the tropical lower atmosphere and solar rotation effect is still a hypothesis and strongly requires to be verified further based on various kinds of observations (Takahashi et al. 2010). Overall, the solar activity is not intense because the year of 2006 is in the late declining phase of solar cycle 23, and there is not a clear corresponding relation between the quasi-27-day periodicity in the zonal wind of the MLT and the solar rotation effect. In other words, the quasi-27-day ISO originates from the tropical convective activity and then is reprinted in the MLT through wave coupling.

Summary

The meteor radar observation indicates that the quasi-27-day oscillation in the MLT arises as a case event rather than a persistent phenomenon, and takes place only once in 1-year observation. By combining the meteor radar and radiosonde measurements and the MERRA-2 reanalysis data for 81 days from 12 August to 31 October 2006, we study the quasi-27-day ISO event in the tropical zonal wind from the troposphere to the MLT.

The radiosonde observations at the three tropical stations distributed in the NH and SH show that the quasi-27-day oscillation originates from the lower atmosphere, and has an amplitude of about $7\text{--}8\text{ ms}^{-1}$ in the zonal wind in the upper troposphere. Above the tropopause, the oscillation attenuates rapidly, which is in agreement with most previous observations. The reanalysis data indicate that the quasi-27-day oscillation is strengthened in the upper stratosphere, and attains a magnitude of about 11 ms^{-1} . The ISO enhancement in the stratopause region is also reported in early studies. Whereas the oscillation decays quickly again from about 70 km, the meteor radar observation illustrates that the oscillation increases again from about 90 km, and reaches an intensity of about 15 ms^{-1} at 100 km. Hence, the quasi-27-day oscillation exhibits an interesting three-layer structure from the troposphere to the MLT. The oscillation in the MLT is different from the previous observations in which the ISO in the zonal wind of the MLT appears generally in winter with the amplitude peak at about 80–90 km, and then is rapidly weakened with increasing height (Eckermann et al. 1997; Luo et al. 2001; Huang et al. 2015).

In the present study, we make an attempt to look into the possible scenario of the generation of the triple-layered quasi-27-day oscillation. As proxies of convection activity, the OLR and specific humidity observations demonstrate that there is a quasi-27-day periodicity in the convective activity in the tropics. The convection is a main excitation source of tropical ISOs and waves, thus the quasi-27-day variability takes place not only in the wind field in the troposphere, but also in the convectively modulated GW activity. As the GWs propagate upward, they can be modulated by the zonal wind oscillation in the upper troposphere. Hence, the quasi-27-day variability in the GW activity has a sharper spectrum in the lower stratosphere relative to that in the troposphere, even though the zonal wind in the lower stratosphere does not display a quasi-27-day ISO. The latitudinal evolution of the oscillation phase derived from the reanalysis data shows that in the upper stratosphere, the quasi-27-day oscillation propagates from the mid-latitudes of both the SH and NH to the low latitudes of the NH. The oscillation may be strengthened by means of the absorption of the GW

momentum and energy through the critical level filtering. The oscillation is in-phase between the upper troposphere and the upper stratosphere, meaning that the GWs are modulated further in the upper stratosphere. As the modulated GWs propagate upward to higher altitudes, they induce the quasi-27-day variability in the zonal wind of the MLT through their momentum and energy deposition due to instability and dissipation. Therefore, the quasi-27-day oscillation in the MLT has the opposite phase relationship with that in the lower atmosphere, and GWs play an important role in the connection of the quasi-27-day oscillation between the lower atmosphere and the MLT.

We investigate the relation between the 27-day oscillation in the MLT and the solar rotation effect. The Lyman- α flux and F10.7 of solar radiation show the quasi-27-day periodicity during April–June and November–December in 2006, respectively, whereas the quasi-27-day ISO in the MLT occurs only during August–October, 2006, indicating that there is not a clear corresponding relation between the quasi-27-day variability in the MLT and the solar rotation periodicity. Since a 27-day variability in the wind and temperature may be an inherent feature of the atmosphere, the quasi-27-day oscillation originated from the tropical convective activity can arise in the MLT through the wave coupling and propagates in the MLT.

Acknowledgements

We are grateful to the editor and anonymous reviewers for their valuable comments on our paper. We thank the NOAA for providing the radiosonde data, OLR and the F10.7, the LASP, University of Colorado for providing the Lyman- α flux, and the NASA for providing the MERRA-2 data.

Authors' contributions

KH and HC proposed the scientific ideas. HC and KH completed the analysis and the manuscript. AZL, SZ, CH and YG discussed the results in the manuscript. All authors read and approved the final manuscript.

Funding

This work was jointly supported by the National Natural Science Foundation of China under Grant Numbers 41974176 and 41674151.

Availability of data and materials

The radiosonde data are available from the websites at <ftp://ftp.ncdc.noaa.gov>; the OLR at <https://www.esrl.noaa.gov/psd/>; the F10.7 at <https://www.ngdc.noaa.gov>; the Lyman- α flux at <http://lasp.colorado.edu/lisird/>; and the MERRA-2 data at <https://disc.gsfc.nasa.gov/datasets>.

Declarations

Competing interests

The authors declare that they have no competing interests.

Author details

¹School of Electronic Information, Wuhan University, Wuhan 430072, China.

²Key Laboratory of Geospace Environment and Geodesy, Ministry of Education, Wuhan, China. ³State Observatory for Atmospheric Remote Sensing, Wuhan, China. ⁴Department of Physical Science, Embry-Riddle Aeronautical University, Daytona Beach, FL, USA.

Received: 9 June 2021 Accepted: 19 September 2021
Published online: 11 October 2021

References

- Alduchov OA, Eskridge RE (1996) Improved magnus form approximation of saturation vapor pressure. *J Appl Meteor* 35:601–609.
- Allen SJ, Vincent RA (1995) Gravity wave activity in the lower atmosphere: seasonal and latitudinal variations. *J Geophys Res Atmos* 100:1327–1350. <https://doi.org/10.1029/94JD02688>
- Arkin PA, Ardanuy PE (1989) Estimating climatic-scale precipitation from space: a review. *J Clim* 2:1229–1238. [https://doi.org/10.1175/1520-0442\(1989\)002%3c1229:ECSPF5%3e2.0.CO;2](https://doi.org/10.1175/1520-0442(1989)002%3c1229:ECSPF5%3e2.0.CO;2)
- Baldwin MP, Gray LJ, Dunkerton TJ, Hamilton K, Haynes PH, Randel WJ et al (2001) The quasi-biennial oscillation. *Rev Geophys* 39(2):179–229. <https://doi.org/10.1029/1999RG000073>
- Barnes HC, Houze RA Jr (2013) The precipitating cloud population of the Madden-Julian oscillation over the Indian and west Pacific Oceans. *J Geophys Res Atmos* 118:6996–7023. <https://doi.org/10.1002/jgrd.50375>
- Coley WR, Heelis RA (2012) Response of the equatorial topside ionosphere to 27-day variations in solar EUV input during a low solar activity period using C/NOFS. *J Geophys Res Space Phys* 117:A03330. <https://doi.org/10.1029/2011JA017301>
- Dunkerton TJ (1997) The role of gravity waves in the quasi-biennial oscillation. *J Geophys Res Atmos* 102:26053–26076. <https://doi.org/10.1029/96JD02999>
- Eckermann SD, Vincent RA (1994) First observations of intraseasonal oscillations in the equatorial mesosphere and lower thermosphere. *Geophys Res Lett* 21:265–268. <https://doi.org/10.1029/93GL02835>
- Eckermann SD, Rajopadhyaya DK, Vincent RA (1997) Intraseasonal wind variability in the equatorial mesosphere and lower thermosphere: long-term observations from the central Pacific. *J Atmos and Sol Terr Phys* 59:603–627. [https://doi.org/10.1016/S1364-6826\(96\)00143-5](https://doi.org/10.1016/S1364-6826(96)00143-5)
- Fioletov VE (2009) Estimating the 27-day and 11-year solar cycle variations in tropical upper stratospheric ozone. *J Geophys Res Atmos* 114:D02302. <https://doi.org/10.1029/2008JD010499>
- Franke SJ, Chu X, Liu AZ, Hocking WK (2005) Comparison of meteor radar and Na Doppler lidar measurements of winds in the mesopause region above Maui Hawaii. *J Geophys Res Atmos* 110:D09502. <https://doi.org/10.1029/2003JD004486>
- Fritts DC, Alexander MJ (2003) Gravity wave dynamics and effects in the middle atmosphere. *Rev Geophys* 41(1):1003. <https://doi.org/10.1029/2001RG000106>
- Gelaro R, McCarty W, Suárez MJ, Todling R, Molod A, Takacs L et al (2017) The modern-era retrospective analysis for research and applications, version 2 (MERRA-2). *J Clim* 30:5419–5454. <https://doi.org/10.1175/JCLI-D-16-0758.1>
- Guharay A, Batista PP, Clemesha BR, Sarkhel S, Buriti RA (2014) Investigation of the intraseasonal oscillations over a Brazilian equatorial station: a case study. *Earth Planets Space* 66:145. <https://doi.org/10.1186/s40623-014-0145-3>
- Guharay A, Batista PP, Buriti RA, Schuch NJ (2017) Signature of the quasi-27-day oscillation in the MLT and its relation with solar irradiance and convection. *J Atmos and Sol Terr Phys* 161:1–7. <https://doi.org/10.1016/j.jastp.2017.06.001>
- Hocking WK, Fuller B, Vandeppeer B (2001) Real-time determination of meteor-related parameters utilizing modern digital technology. *J Atmos Sol Terr Phys* 63:155–169. [https://doi.org/10.1016/S1364-6826\(00\)00138-3](https://doi.org/10.1016/S1364-6826(00)00138-3)
- Hoffmann CG, von Savigny C (2019) Indications for a potential synchronization between the phase evolution of the Madden-Julian oscillation and the solar 27-day cycle. *Atmos Chem Phys* 19:4235–4256. <https://doi.org/10.5194/acp-19-4235-2019>
- Hood LL (2016) Lagged response of tropical tropospheric temperature to solar ultraviolet variations on intraseasonal time scales. *Geophys Res Lett* 43(8):4066–4075. <https://doi.org/10.1002/2016GL068855>
- Huang KM, Liu AZ, Lu X, Li Z, Gan Q, Gong Y et al (2013a) Nonlinear coupling between quasi 2 day wave and tides based on meteor radar observations at Maui. *J Geophys Res Atmos* 118:10936–10943. <https://doi.org/10.1002/jgrd.50872>
- Huang KM, Liu AZ, Zhang SD, Yi F, Huang CM, Gan Q et al (2013b) A nonlinear interaction event between a 16-day wave and a diurnal tide from meteor radar observations. *Ann Geophys* 31:2039–2048. <https://doi.org/10.5194/angeo-31-2039-2013>
- Huang KM, Liu AZ, Zhang SD, Yi F, Huang CM, Gan Q et al (2015) Observational evidence of quasi-27-day oscillation propagating from the lower atmosphere to the mesosphere over 20° N. *Ann Geophys* 33:1321–1330. <https://doi.org/10.5194/angeo-33-1321-2015>
- Huang KM, Yang ZX, Wang R, Zhang SD, Huang CM, Yi F, Hu F (2018) A statistical study of inertia gravity waves in the lower stratosphere over the Arctic region based on radiosonde observations. *J Geophys Res Atmos* 123:4958–4976. <https://doi.org/10.1029/2017JD027998>
- Huang KM, Xi Y, Wang R, Zhang SD, Huang CM, Gong Y et al (2019) Signature of a quasi 30-day oscillation at midlatitude based on wind observations from MST radar and meteor radar. *J Geophys Res Atmos* 124:11266–11280. <https://doi.org/10.1029/2019JD031170>
- Isoda F, Tsuda T, Nakamura T, Vincent RA, Reid IM, Achmad E et al (2004) Intraseasonal oscillations of the zonal wind near the mesopause observed with medium-frequency and meteor radars in the tropics. *J Geophys Res Atmos* 109:D21108. <https://doi.org/10.1029/2003JD003378>
- Karmakar N, Krishnamurti TN (2019) Characteristics of northward propagating intraseasonal oscillation in the Indian summer monsoon. *Clim Dyn* 52:1903–1916. <https://doi.org/10.1007/s00382-018-4268-2>
- Kumar K, Jain AR (1994) Latitudinal variations of 30–70 day period waves over the tropical Indian zone. *J Atmos Terr Phys* 56:1135–1145. [https://doi.org/10.1016/0021-9169\(94\)90052-3](https://doi.org/10.1016/0021-9169(94)90052-3)
- Kumar KK, Antonita TM, Ramkumar G, Deepa V, Gurubaran S, Rajaram R (2007) On the tropospheric origin of mesosphere lower thermosphere region intraseasonal wind variability. *J Geophys Res Atmos* 112:D07109. <https://doi.org/10.1029/2006JD007962>
- Lau K-M, Peng L (1990) Origin of low frequency (intraseasonal) oscillations in the tropical atmosphere. Part III: monsoon dynamics. *J Atmos Sci* 47:1443–1462. [https://doi.org/10.1175/1520-0469\(1990\)047%3c1443:OOLF0I%3e2.0.CO;2](https://doi.org/10.1175/1520-0469(1990)047%3c1443:OOLF0I%3e2.0.CO;2)
- Li Z, Li Y, Bonsal B, Manson AH, Scaff L (2018) Combined impacts of ENSO and MJO on the 2015 growing season drought on the Canadian Prairies. *Hydrol Earth Syst Sci* 22:5057–5067. <https://doi.org/10.5194/hess-22-5057-2018>
- Liebmann B, Smith CA (1996) Description of a complete (interpolated) outgoing longwave radiation dataset. *Bull Am Meteorol Soc* 77:1275–1277
- Lindzen RS (1981) Turbulence and stress owing to gravity wave and tidal breakdown. *J Geophys Res Oceans* 86:9707–9714. <https://doi.org/10.1029/JC086iC10p09707>
- Liu AZ, Lu X, Franke SJ (2013) Diurnal variation of gravity wave momentum flux and its forcing on the diurnal tide. *J Geophys Res Atmos* 118:1668–1678. <https://doi.org/10.1029/2012JD018653>
- Luo Y, Manson AH, Meek CE, Igarashi K, Jacobi C (2001) Extra long period (20–40 day) oscillations in the mesospheric and lower thermospheric winds: observations in Canada, Europe and Japan, and considerations of possible solar influences. *J Atmos Sol Terr Phys* 63:835–852. [https://doi.org/10.1016/S1364-6826\(00\)00206-6](https://doi.org/10.1016/S1364-6826(00)00206-6)
- Madden RA (1986) Seasonal variations of the 40–50 day oscillation in the tropics. *J Atmos Sci* 43:3138–3158. [https://doi.org/10.1175/1520-0469\(1986\)043%3c3138:SVOTDO%3e2.0.CO;2](https://doi.org/10.1175/1520-0469(1986)043%3c3138:SVOTDO%3e2.0.CO;2)
- Madden RA, Julian PR (1971) Detection of a 40–50 day oscillation in the zonal wind in the tropical Pacific. *J Atmos Sci* 28:702–708. [https://doi.org/10.1175/1520-0469\(1971\)028%3c0702:DOADOI%3e2.0.CO;2](https://doi.org/10.1175/1520-0469(1971)028%3c0702:DOADOI%3e2.0.CO;2)
- Madden RA, Julian PR (1994) Observations of the 40–50-day tropical oscillation—a review. *Mon Wea Rev* 122:814–837. [https://doi.org/10.1175/1520-0493\(1994\)122%3c0814:OOTDIO%3e2.0.CO;2](https://doi.org/10.1175/1520-0493(1994)122%3c0814:OOTDIO%3e2.0.CO;2)
- Moss AC, Wright CJ, Mitchell NJ (2016) Does the Madden-Julian oscillation modulate stratospheric gravity waves? *Geophys Res Lett* 43:3973–3981. <https://doi.org/10.1002/2016GL068498>
- Nagpal OP, Dhaka SK, Srivastav SK (1994) Wave characteristics in the troposphere and stratosphere over the Indian tropics during the DYANA period. *J Atmos Terr Phys* 56:1117–1133. [https://doi.org/10.1016/0021-9169\(94\)90051-5](https://doi.org/10.1016/0021-9169(94)90051-5)
- Niranjan Kumar K, Ramkumar TK, Krishnaiah M (2011) Vertical and lateral propagation characteristics of intraseasonal oscillation from the tropical lower troposphere to upper mesosphere. *J Geophys Res Atmos* 116:D21112. <https://doi.org/10.1029/2010JD015283>

- Ogino S-Y, Yamanaka MD, Shibagaki Y, Shimomai Y, Fukao S (1998) Horizontal variations of gravity wave activities in the lower stratosphere over Japan: a case study in the Baiu season 1991. *Earth Planets Space* 51:107–113. <https://doi.org/10.1186/BF03352215>
- Pancheva D, Schminder R, Laštovička J (1991) 27-day fluctuations in the ionospheric D-region. *J Atmos Terr Phys* 53:1145–1150. [https://doi.org/10.1016/0021-9169\(91\)90064-E](https://doi.org/10.1016/0021-9169(91)90064-E)
- Pancheva D, Mitchell NJ, Younger PT, Muller HG (2003) Intra-seasonal oscillations observed in the MLT region above UK (52°N, 2°W) and ESRANGE (68°N, 21°E). *Geophys Res Lett* 30:2084. <https://doi.org/10.1029/2003GL017809>
- Rao RK, Gurubaran S, Sathishkumar S, Sridharan S, Nakamura T, Tsuda T et al (2009) Longitudinal variability in intraseasonal oscillation in the tropical mesosphere and lower thermosphere region. *J Geophys Res Atmos* 114:D19110. <https://doi.org/10.1029/2009JD011811>
- Ratnam MV, Alexander SP, Kozu T, Tsuda T (2009) Characteristics of gravity waves observed with intensive radiosonde campaign during November–December 2005 over western Sumatera. *Earth Planets Space* 61:983–993. <https://doi.org/10.1186/BF03352948>
- Reed RJ, Campbell WJ, Rasmussen LA, Rogers DG (1961) Evidence of a downward-propagating, annual wind reversal in the equatorial stratosphere. *J Geophys Res* 66:813–818. <https://doi.org/10.1029/JZ066i003p00813>
- Rich FJ, Sultan PJ, Burke WJ (2003) The 27-day variations of plasma densities and temperatures in the topside ionosphere. *J Geophys Res Space Physics* 108:1297. <https://doi.org/10.1029/2002JA009731>
- Salby ML, Garcia RR, Hendon HH (1994) Planetary-scale circulations in the presence of climatological and wave-induced heating. *J Atmos Sci* 51:2344–2367. [https://doi.org/10.1175/1520-0469\(1994\)051%3c2344:PSCITP%3e2.0.CO;2](https://doi.org/10.1175/1520-0469(1994)051%3c2344:PSCITP%3e2.0.CO;2)
- Sato K, Nomoto M (2015) Gravity wave-induced anomalous potential vorticity gradient generating planetary waves in the winter mesosphere. *J Atmos Sci* 72(9):3609–3624. <https://doi.org/10.1175/JAS-D-15-0046.1>
- Sato K, Watanabe S, Kawatani Y, Tomikawa Y, Miyazaki K, Takahashi M (2009) On the origins of mesospheric gravity waves. *Geophys Res Lett* 36:L19801. <https://doi.org/10.1029/2009GL039908>
- Scargle JD (1982) Studies in astronomical time series analysis. II. Statistical aspects of spectral analysis of unevenly spaced data. *Astrophys J* 263:835–853
- Schanz A, Hocke K, Kämpfer N (2016) On forced and free atmospheric oscillations near the 27-day periodicity. *Earth Planets Space* 68:97. <https://doi.org/10.1186/s40623-016-0460-y>
- Smith AK (2003) The origin of stationary planetary waves in the upper mesosphere. *J Atmos Sci* 60:3033–3041. [https://doi.org/10.1175/1520-0469\(2003\)060%3c3033:TOOSPW%3e2.0.CO;2](https://doi.org/10.1175/1520-0469(2003)060%3c3033:TOOSPW%3e2.0.CO;2)
- Sukhodolov T, Rozanov E, Ball WT, Peter T, Schmutz W (2017) Modeling of the middle atmosphere response to 27-day solar irradiance variability. *J Atmos Sol Terr Phys* 152:50–61. <https://doi.org/10.1016/j.jastp.2016.12.004>
- Takahashi Y, Okazaki Y, Sato M, Miyahara H, Sakanoi K, Hong PK et al (2010) 27-day variation in cloud amount in the Western Pacific warm pool region and relationship to the solar cycle. *Atmos Chem Phys* 10:1577–1584. <https://doi.org/10.5194/acp-10-1577-2010>
- Thiéblemont R, Bekki S, Marchand M, Bossay S, Schmidt H, Meftah M et al (2018) Nighttime mesospheric/lower thermospheric tropical ozone response to the 27-day solar rotational cycle: ENVISAT-GOMOS satellite observations versus HAMMONIA idealized chemistry-climate model simulations. *J Geophys Res Atmos* 123:8883–8896. <https://doi.org/10.1029/2017JD027789>
- Tsuchiya C, Sato K, Alexander MJ, Hoffmann L (2016) MJO-related intraseasonal variation of gravity waves in the southern Hemisphere tropical stratosphere revealed by high-resolution AIRS observations. *J Geophys Res Atmos* 121:7641–7651. <https://doi.org/10.1002/2015JD024463>
- Tsuda T, Ratnam MV, Alexander SP, Kozu T, Takayabu Y (2009) Temporal and spatial distributions of atmospheric wave energy in the equatorial stratosphere revealed by GPS radio occultation temperature data obtained with the CHAMP satellite during 2001–2006. *Earth Planets Space* 61:525–533. <https://doi.org/10.1186/BF03353169>
- Vincent RA, Alexander MJ (2000) Gravity waves in the tropical lower stratosphere: an observational study of seasonal and interannual variability. *J Geophys Res Atmos* 105:17971–17982. <https://doi.org/10.1029/2000JD900196>
- Xu J, Wang W, Lei J, Sutton EK, Chen G (2011) The effect of periodic variations of thermospheric density on CHAMP and GRACE orbits. *J Geophys Res Space Phys* 116:A02315. <https://doi.org/10.1029/2010JA015995>
- Yamanaka MD, Ogino S, Kondo S, Shimomai T, Fukao S, Shibagaki Y et al (1996) Inertio-gravity waves and subtropical multiple tropopauses: vertical wavenumber spectra of wind and temperature observed by the MU radar, radiosondes and operational rawinsonde network. *J Atmos Terr Phys* 58(6):785–805. [https://doi.org/10.1016/0021-9169\(95\)00074-7](https://doi.org/10.1016/0021-9169(95)00074-7)
- Yoshida S, Tsuda T, Shimizu A, Nakamura T (1999) Seasonal variations of 3.0–3.8-day ultra-fast Kelvin waves observed with a meteor wind radar and radiosonde in Indonesia. *Earth Planets Space* 51:675–684. <https://doi.org/10.1186/BF03353225>
- Zhang C (2005) Madden–Julian oscillation. *Rev Geophys* 43:RG2003. <https://doi.org/10.1029/2004RG000158>
- Zhang SD, Yi F (2007) Latitudinal and seasonal variations of inertial gravity wave activity in the lower atmosphere over central China. *J Geophys Res Atmos* 112:D05109. <https://doi.org/10.1029/2006JD007487>
- Zhang SD, Yi F, Huang CM, Huang KM (2012) High vertical resolution analyses of gravity waves and turbulence at a midlatitude station. *J Geophys Res Atmos* 117:D02103. <https://doi.org/10.1029/2011JD016587>
- Ziemke JR, Stanford JL (1991) One-to-two month oscillations: observed high-latitude tropospheric and stratospheric response to tropical forcing. *J Atmos Sci* 48:1336–1347. [https://doi.org/10.1175/1520-0469\(1991\)048%3c1336:OTTMOO%3e2.0.CO;2](https://doi.org/10.1175/1520-0469(1991)048%3c1336:OTTMOO%3e2.0.CO;2)

Publisher's Note

Springer Nature remains neutral with regard to jurisdictional claims in published maps and institutional affiliations.

Submit your manuscript to a SpringerOpen® journal and benefit from:

- Convenient online submission
- Rigorous peer review
- Open access: articles freely available online
- High visibility within the field
- Retaining the copyright to your article

Submit your next manuscript at ► [springeropen.com](https://www.springeropen.com)